PROTEINS: Structure, Function, and Genetics 15:80–87 (1993)

Crystallographic Analysis of Thr-200 → His Human Carbonic Anhydrase II and Its Complex With the Substrate, HCO_3^-

Yafeng Xue,[1] Jukka Vidgren,[2] L. Anders Svensson,[2] Anders Liljas,[2] Bengt-Harald Jonsson,[1] and Sven Lindskog[1]

[1]Department of Biochemistry, University of Umeå, S-90187 Umeå, Sweden and [2]Department of Molecular Biophysics, Chemical Center, University of Lund, S-22100 Lund, Sweden

ABSTRACT **A complex of carbonic anhydrase (CA) with one of its substrates, bicarbonate, has been studied crystallographically. Human isoenzyme II was mutated at position 200 from threonine to histidine, which results in higher affinity for bicarbonate. The HCO_3^- ion binds in the active site to the zinc ion as a pseudo-bidentate ligand which gives the metal a coordination geometry between tetrahedral and trigonal bipyramide. The water/hydroxide normally bound with tetrahedral coordination to the zinc is probably replaced by the OH group of the bicarbonate ion. The importance of residues Thr-199 and Glu-106 in controlling the binding orientation of HCO_3^- is discussed as well as the catalytic mechanism. Both the complex as well as the uncomplexed mutant were studied at 1.9 Å resolution.** © 1993 Wiley-Liss, Inc.

Key words: refined structures, mutant, substrate binding, zinc coordination

INTRODUCTION

The zinc metalloenzyme carbonic anhydrase (CA) catalyzes the reversible hydration of carbon dioxide to bicarbonate. It is widely accepted that the initial step of the reaction is a nucleophilic attack by a zinc-bound hydroxide ion on carbon dioxide. In CA II, the catalytically most efficient isoenzyme form, the hydroxide ion is generated by proton transfer from a zinc bound water molecule to a buffer molecule via a proton shuttle group, which has been identified as His-64.[1–3] Although the postulated mechanism implies that the substrate is bound in close vicinity of the metal ion, no crystallographic observation of a substrate bound to the active site of CA has so far been made. A major reason for this is the low substrate binding affinity of isoenzyme II.

Among the different isoenzymes, all sequenced type I CA:s have histidine at position 200. This is the only unique active site feature that clearly distinguishes isoenzymes I from type II CA:s, where a threonine is usually found in position 200.[4,5] The kinetic properties of the Thr-200 → His (T200H) mutant of human isoenzyme II suggest that His-200 is an important determinant of the specific catalytic behavior of isoenzyme I.[6] Bicarbonate as well as other monovalent anions bind more strongly to CA:s I or to this mutant than to CA:s II.[5,6] In fact, at pH near 8 where most crystallographic investigations have been made and where HCO_3^- is the predominating species of the carbonate system, the mutant has an even higher HCO_3^- affinity than human isoenzyme I.[6]

In the study presented in this paper we have utilized this property of Thr-200 → His human CA II to obtain, for the first time, the crystal structure of a carbonic anhydrase–substrate complex.

EXPERIMENTAL PROCEDURES

The Thr-200 → His mutant of human CA II has been described earlier.[6] It was purified by affinity chromatography according to the procedure of Khalifah et al.[7] However, an additional ion-exchange chromatography step (S-Sepharose Fast Flow, Pharmacia) was included and resulted in improved crystal quality.

Crystals of the mutant enzyme were grown by the hanging drop method using 2.3 M $(NH_4)_2SO_4$ in 50 mM Tris-H_2SO_4 buffer, pH 8.5, containing 4 mM dithiothreitol or methylmercuric chloride in a 1:4 molar enzyme/CH_3HgCl ratio.[8] The dithiothreitol or the methylmercuric chloride served to prevent formation of intermolecular disulfide bridges. Crystals of the HCO_3^- complex of the mutant were obtained by soaking crystals of the uncomplexed protein in a solution containing 2.3 M $(NH_4)_2SO_4$ in 50 mM Tris-H_2SO_4 buffer, pH 7.8, and 0.8 M NH_4HCO_3. No special effort was made to remove the methylmercuric chloride.

X-ray intensity data were collected using a Siemens (Xentronics) multiwire area detector mounted on a Rigaku RU200HB rotating anode generator (CuK_α radiation, 0.3 × 3 mm focal spot, graphite

Received January 9, 1992; revision accepted April 6, 1992.
Address reprint requests to Dr. Anders Liljas, Department of Molecular Biophysics, Chemical Center, the University of Lund, P.O. Box 124, S-22100 Lund, Sweden.

TABLE I. Data Collection and Refinement Statistics

	T200H	Complex
Data collection		
Resolution (Å)	1.9	1.9
Refinement R-value (%)	15.5	14.6
Error in coordinates (Å) according to Luzzatti plot	0.16	0.16
Observations	41,574	28,334
Independent reflexions	17,962	15,298
Completeness (%)	89	77
R_{merge} (%)	6.6	7.0
Refinement		
Reflections used ($F>$<2$\sigma(F)>$)	16,980	14,437
Protein atoms	2,072	2,078
Solvent atoms	218	214
rms values		
Bond distance (Å)	0.018	0.014
Angle distance (Å)	0.034	0.032
Planar 1–4 distance (Å)	0.047	0.041
Plane groups (Å)	0.017	0.014
Chiral centers (Å^3)	0.186	0.171
Single torsion (Å)	0.157	0.157
Multiple torsion (Å^3)	0.160	0.161
Possible X–Y H-bond (Å)	0.155	0.159
Torsion angles		
Planar (°)	3.1	2.7
Staggered (°)	15.9	16.7
Orthonormal (°)	30.3	30.7
Thermal restraints		
Main chain bond (Å^2)	0.880	0.763
Main chain angle (Å^2)	1.422	1.278
Side chain bond (Å^2)	1.820	1.506
Side chain angle (Å^2)	2.846	2.371

monochromator). The detector was placed 8.0 cm from the crystal (8.5 cm for the complex). The Siemens 3 axis goniostat with a fixed $\chi = 45°$ was used with $2\theta = 20°$ (23° for the complex). The crystal was rotated 180° about ω with a step size of 0.30° (0.25° for the complex) and an exposure time of 90 sec per frame. The total data were collected from a single crystal during about 36 hr for both data sets. The reflection data were integrated, reduced, merged, and scaled using the XENGEN program suite.[9] Further details about the data collection are given in Table I.

All calculations were done on a VAX workstation 3100. The $2|F_{obs}|-|F_{calc}|$ and $|F_{obs}|-|F_{calc}|$ electron density maps were calculated with the CCP4 program package[10] and inspected at several stages of the work on Evans & Sutherland ESV and PS390 graphical stations using the programs FRODO[11,12] and O.[13] Restrained least squares refinement[14] was carried out with the program PROFFT[15] refining both atomic positions and individual temperature factors. The starting model for the refinement was the refined structure of human CA II at 1.6 Å resolution (K. Håkanson, M. Carlsson, A. Svensson, and A. Liljas, J. Mol. Biol., accepted for publication) without the side chain of residue 200 and nine of the active site water molecules. Histidine 200 was subsequently built into the model (based on the electron density maps obtained). In the case of the complex the HCO_3^- was built into the active site after a few cycles of refinement.

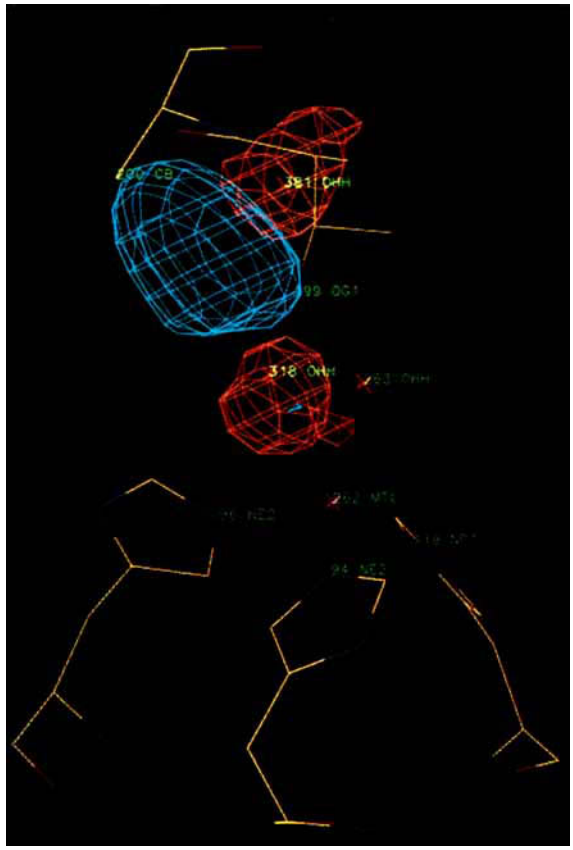

Fig. 1. $|F_o|-|F_c|$ difference map of the Thr-200 → His mutant of human CA II. The phase angles were obtained from the refined coordinates of the mutant enzyme. This map was calculated after deleting the imidazole group and reinserting two of the deleted water molecules (Wat-318 and Wat-381). Contours are drawn at ±3.5 σ.

RESULTS

Structure of Thr-200 → His Human CA II

The refinement was completed with an R factor of 15.5% at 1.9 Å resolution (Table I). A Luzzati plot[16] indicates that the error in the atomic coordinates is around 0.16 Å. The root-mean-square difference in atomic coordinates compared to the original ones is 0.13 Å.

The difference electron density from $|F_{obs}|-|F_{calc}$ (native)| shows no large positive or negative peaks except those associated with the replacement of threonine by histidine at position 200 (Fig. 1). The side chain of His-200 protrudes from one side of the entrance of the active site cavity, with the imidazole

ring pointing into the cavity. Two water molecules (Wat-318 and Wat-381), present in the active site of the wild-type enzyme, have been displaced due to the reduced space. One of them, Wat-318, links the zinc-bound water to the rest of the network of ordered water molecules in wild-type enzyme (Fig. 2A). Thus, it appears that the zinc-bound water is not included in this network in the mutant.

All atoms of residues 200 to 204 have shifted up to 0.5 Å compared to their positions in native human CA II. Two hydrogen bonds seem to define the orientation of the imidazole ring of His-200, one between Nδ1 and the carbonyl oxygen of Pro-201 and another between Nε2 and a water molecule, Wat-359 (Table II), which forms a hydrogen bond with another water molecule, Wat-369 (Fig. 2B). His-64 has a short distance (2.9 Å) to Wat-332 (Table II). We have interpreted this as a rotation of χ^2 by 180° to allow for a hydrogen bond to Nδ1 which is observed neither in the wild-type structure nor in the structure of the complex. The closest distance between the imidazole rings of His-200 and His-64 is 3.9 Å. The addition of the histidine leads to a reduced size of the entrance to the zinc region. One of the ring atoms of His-200 (Cδ2) is 4.7 Å from the zinc ion and 3.4 Å from the zinc-bound H_2O/OH^-. The coordination geometry of the zinc ion remains almost the same as in native human CA II (Table III).

Structure of the HCO_3^- Complex of Thr-200 → His Human CA II

The structure of the complex was refined at 1.9 Å resolution with an R value of 14.6% (Table I). A Luzzati plot[16] indicates that the error in the atomic coordinates is 0.16 Å. The root-mean-square difference with respect to the coordinates of native human CA II is 0.24 Å and with respect to those of the uncomplexed mutant 0.24 Å.

A triangular, planar electron density is clearly seen associated with the zinc ion in the $|F_{obs}|-|F_{calc}|$ Fourier map (Fig. 3). This was interpreted as HCO_3^- and built into the density after a few cycles of refinement. The zinc-bound water molecule, Wat-263, as well as the "deep"[17] water molecule, Wat-338, have been displaced by the HCO_3^- ion (Fig. 2C, Fig. 4).

The coordination geometry of the zinc ion is somewhere between tetrahedral and trigonal bipyramidal (Table III). The HCO_3^- ion is a "pseudo-bidentate" zinc ligand. One oxygen atom from HCO_3^- is located near the position of the original zinc-bound water molecule (shift, 0.42 Å) at a distance of 2.2 Å from the zinc ion and 2.6 Å from Oγ1 of Thr-199. This oxygen atom is in van der Waals' contact with Cδ2 of His-200 (O–C distance, 3.3 Å) and this might partially explain the enhanced affinity of HCO_3^- for the mutant. Another oxygen atom of the HCO_3^- ion is 2.5 Å from the zinc ion and 2.8 Å from one water

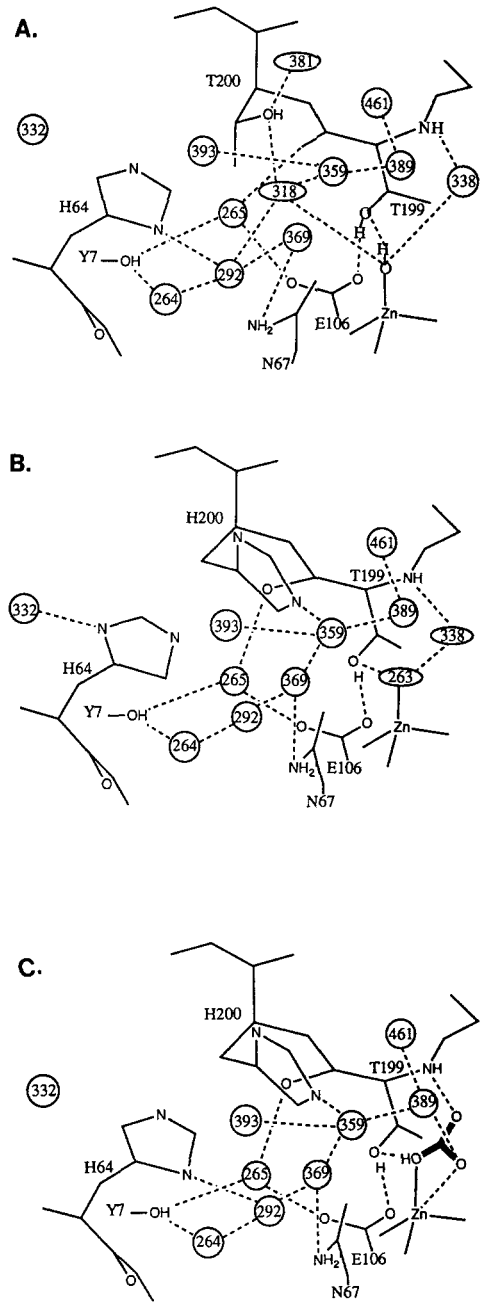

Fig. 2. Schematic drawings of the residues and solvent molecules in the active site. Hydrogen bonds are indicated by dashed lines. The zinc ion is at the lower right. (**A**) The native wild type enzyme. The coordinates are from the work by Håkansson et al. (J. Mol. Biol., accepted for publication). The zinc water/hydroxide ion is connected by hydrogen bonds through water molecules 318 and 292 to His-64, the proton shuttle group. (**B**) The mutant Thr-200 → His. Two water molecules 318 and 381 are displaced by the mutation. There is no connection through hydrogen bonds between the zinc water/hydroxide ion and His-64. The imidazole ring of His-64 appears to have flipped 180° from its conformation in the wild type enzyme (A) as well as in the bicarbonate complex (C). (**C**) The mutant with the bound bicarbonate ion. The substrate displaces the zinc water (263) and the deep water (338) molecules. The OH group is situated 2.2 Å from the zinc ion whereas one of the other oxygens is 2.5 Å from the zinc making the bicarbonate a pseudo-bidentate ligand to the metal. Cδ2 of His-200 is situated 3.3 Å from the oxygen bound at the zinc.

TABLE II. Hydrogen Bond Distances (Å) in the Active Site*

	HCAII	T200H	Complex
263 OHH–318 OHH	2.8	—	—
263 OHH–338 OHH	2.6	2.4	—
263 OHH–Oγl Thr-199	2.8	2.9	—
264 OHH–292 OHH	2.9	2.9	2.8
264 OHH–Oη Tyr-7	2.9	2.8	2.8
265 OHH–Oη Tyr-7	2.6	2.6	2.5
265 OHH–Oϵ2 Glu-106	2.7	2.7	2.8
265 OHH–O Thr-199	2.9	2.8	3.0
292 OHH–318 OHH	2.7	—	—
292 OHH–369 OHH	2.7	2.5	2.6
292 OHH–Nδ1 His-64	3.2	(3.4)	3.1
318 OHH–Oλ1 Thr-200	2.8	—	—
318 OHH–359 OHH	2.6	—	—
332 OHH–Nδ1 His-64	(3.8)	2.9	(3.9)
359 OHH–369 OHH	(3.5)	3.1	2.8
359 OHH–389 OHH	2.6	2.6	2.6
359 OHH–393 OHH	3.0	3.1	3.0
359 OHH–Nϵ2 His-200	—	2.9	2.6
369 OHH–Nδ2 Asn-67	2.8	2.8	2.7
389 OHH–461 OHH	2.6	2.5	2.5
Oϵ1 Gln-92–Nδ1 His-94	2.7	2.7	2.8
Nδ1 His-96–O Asn-244	2.7	2.7	2.7
Oϵ1 Glu-106–Oγ1 Thr-199	2.6	2.5	2.5
Oϵ2 Glu-106–N Arg-246	2.9	2.9	2.9
Oϵ2 Glu-117–Nϵ2 His-119	2.6	2.6	2.6
Nδ1 His-200–O Pro-201	—	2.9	2.8
Cδ2 His-200–263 OHH or O1	—	(3.4)	(3.3)
O1 HCO_3^-–Oγ1 Thr-199	—	—	2.6
O2 HCO_3^-–389 OHH	—	—	2.8
O3 HCO_3^-–N Thr-199	—		3.0

*Information in parentheses does not refer to hydrogen bonds. Note that His-64 has two different conformations (see text).

TABLE III. Zinc Coordination

	Distance (Å)	Angles (°) X-Zn-94	X-Zn-96	X-Zn-119	X-Zn-O2 (HCO_3^-)
A. Geometry of the zinc ion in wild type human CAII*					
OH-263	2.1	111.1	113.4	113.0	
Nϵ2 94	2.1		104.1	115.3	
Nϵ2 96	2.1			99.1	
Nδ1 119	2.1				
B. Geometry of the zinc ion in T200H					
OH-263	2.1	104.0	117.6	111.6	
Nϵ2 94	2.2		106.9	115.0	
Nϵ2 96	2.2			102.1	
Nδ1 119	2.1				
C. Geometry of the zinc ion in T200H/bicarbonate complex					
O1(HCO_3^-)	2.2	117.9	103.5	112.2	55.1
Nϵ2 94	2.2		104.9	117.9	84.0
Nϵ2 96	2.2			96.3	158.1
Nδ1 119	2.2				97.0
O2(HCO_3^-)	2.5				

*Coordinates from Håkansson et al., J. Mol. Biol., accepted for publication.

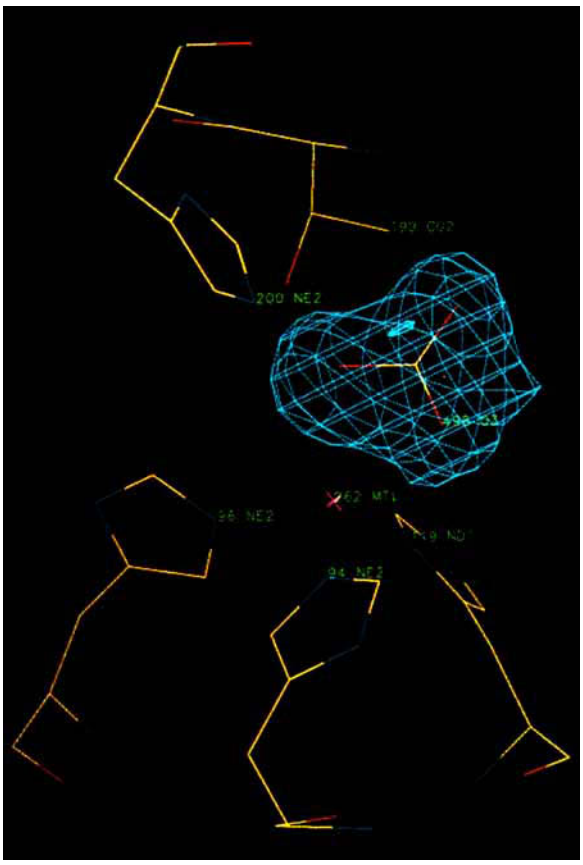

Fig. 3. $|F_o|-|F_c|$ difference map of the Thr-200 → His mutant in complex with HCO_3^-. The phase angles were calculated as described in Figure 1 after deleting the bicarbonate ion. The contours were drawn at $+3.5\sigma$.

molecule, Wat-389, which, furthermore, is connected to the Nε2 atom of His-200 via another water molecule, Wat-359. The third O of HCO_3^- is 3.0 Å from the amide N of Thr-199, close to the position where the "deep" water usually is located (shift, 0.67 Å).

It appears that the imidazole ring of His-64 has flipped around 180° and moved in toward the zinc region compared to its position in the uncomplexed mutant with a shift of about 0.56 Å. The Nδ1 atom is hydrogen bonded to Wat-292 (Fig. 2C), whereas the other ring atoms have no neighbors within hydrogen bond distance.

DISCUSSION

It is now generally accepted that the reversible hydration catalyzed by CA II follows the "zinc-hydroxide" mechanism, which consists of two partial reaction sequences, a CO_2/HCO_3^- interconversion sequence as outlined in Eq. (1) and a proton transfer sequence involving a "proton shuttle group" and a buffer-dependent step as shown in Eq. (2).[1] In Eq. (2), ^+H to the left of E symbolizes a protonated shuttle group, which has been shown to be His-64.[1-3] There is strong evidence that Eq. (1) applies also to CA I,[18] while recent data suggest that proton shuttling is much less prominent in this isoenzyme than in CA II and that additional proton transfer pathways operate.[19]

$$E-OH^- + CO_2 \rightarrow E-HCO_3^- \xrightarrow{H_2O} E-H_2O + HCO_3^- \quad (1)$$

$$E-H_2O \rightarrow {}^+H-E-OH^- \xrightarrow[BH^+]{B} E-OH^- + H_2O \quad (2)$$

The mutant Thr-200 → His human CA II was made to test the hypothesis[5] that His-200 is critically important for the specific functional properties of CA I. The results of an extensive study[6] showed that the mutant is a relatively good mimic of CA I with respect to CO_2/HCO_3^- interconversion, whereas proton transfer appears to proceed efficiently according to Eq. (2) as in wild-type CA II.

A comparison of the crystal structures of human CA I[20] (the coordinates were obtained from the Brookhaven Protein Data Bank[21,22] entry 2CAB) and the Thr-200 → His mutant of CA II shows that there are several basic similarities. For example, the orientations of the side chain of His-200 are virtually identical. The closest distances between the imidazole ring of His-200 and zinc ion is 4.7 Å in the mutant and 5.1 Å in CA I.[20] Furthermore, the shortest distances between His-200 and His-64 are identical in both enzyme forms (4.0 Å).

The position of the imidazole ring of His-64 is almost the same in wild-type CA I and CA II as well as in the mutant. However, the hydrogen bonding pattern in the uncomplexed mutant is compatible with a 180° rotation of the imidazole ring about χ^2 (Fig. 2). In the HCO_3^- complex, His-64 appears to have the same orientation as in wild-type CA II (Fig. 2). The conformational sensitivity of His-64 has recently been demonstrated by Krebs et al.,[23] who found that the side chain has rotated away from the active site by 105° about χ^1 in the crystal structure of a Thr-200 → Ser mutant of human CA II. Subsequently, in other forms of the enzyme, a second minor conformation of His-64, corresponding to that observed in the Thr-200 → Ser mutant, has been detected (ref. 24 and Håkansson et al., J. Mol. Biol., accepted for publication). Moreover, in the crystal structure of a Thr-199 → Ala mutant of human CA II, the two conformations of His-64 are present with about equal occupancies (Y. Xue et al., unpublished results). Thus it appears that the dominating orientation of this residue is under remote control, probably through the variable, water-linked hydrogen-bond network in the active-site cavity. In the two structures studied here only one location of His-64 was observed.

Previously, NMR linewidth data were taken as in-

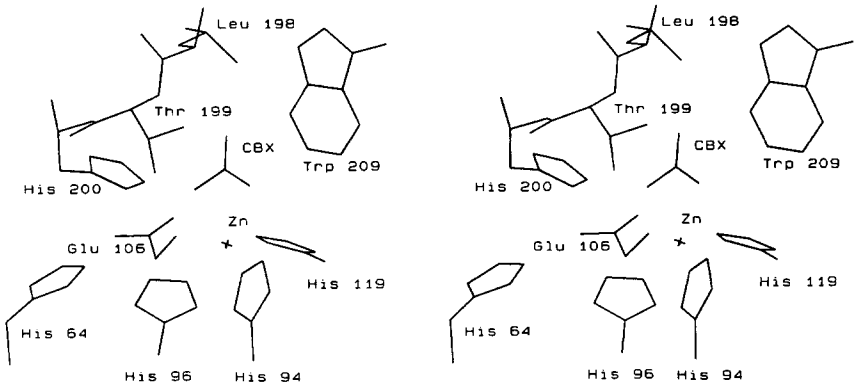

Fig. 4. A stereo diagram of the Thr-200 → His mutant in complex with HCO_3^-. A number of residues in the active site are included, among them His-200 and His-64. Cδ2 of His-200 is in van der Waals contact with the bicarbonate oxygen closest to the zinc ion.

dications that the imidazole ring of His-64 is highly mobile in CA II.[25] Presumably, this mobility is important for the role of His-64 as a proton shuttle in CA II.[1] In unmodified human CA II, the pK_a of His-64 is 7.1,[25] and this is also quite important since efficient proton shuttling at physiological conditions requires the shuttle group to accept as well as donate protons rapidly. In the Thr-200 → His mutant, the pK_a of His-64 is 6.9 and proton shuttling appears unimpaired.[6] In the human CA I framework, which includes other isoenzyme I-specific residues in addition to His-200 for example, His-67 and Val-62, His-64 has a pK_a of 4.7[26] and appears to be less accessible to extraneous buffer molecules than in CA II. Studies of a variety of mutants of human CA II (Z. Liang and S. Lindskog, unpublished results) suggest that His-64 is ideally posed in the active site of CA II to act as an efficient proton shuttle and that histidines in other positions, including 67 and 200, are rather inefficient in this role.

It has been proposed[1] that proton transfer between the zinc-bound water and His-64 proceeds along the chain of water molecules linking donor and acceptor in wild-type CA II (Fig. 2A). In the Thr-200 → His mutant, this chain is interrupted (Fig. 2B), and we conclude that an intact chain of ordered water molecules is not required for efficient proton shuttling.

The most important result presented in this paper is the mode of binding of HCO_3^- in the active site of a catalytically competent form of CA. Although a coordination of HCO_3^- to the metal ion has previously been inferred from a variety of data,[5] very little direct evidence pertaining to this problem is available in the literature. The properties of the absorbtion spectrum of the HCO_3^- complex of cobalt(II)-substituted bovine CA II have been interpreted as due to a thermal equilibrium between four- and five-coordinated species by Bertini et al.[27] From ^{13}C NMR linewidths and spin-lattice relaxation times, Williams and Henkens[28] estimated that the carbon atom of bound HCO_3^- is located 3.2 Å from the metal ion in cobalt(II)-substituted human CA I. The results of Williams and Henkens[28] are compatible with a tetrahedral metal ion coordination sphere and a monodentate binding of HCO_3^-. Led and Nesgaard[29] calculated from NMR data a corresponding distance of 2.7 Å for Mn(II) human CA I and proposed a bidentate coordination of HCO_3^-. However, these distance calculations are sensitive to errors and approximations in theory. Furthermore, it should be pointed out that the Co(II)-substituted enzyme is functionally very similar to native CA whereas the Mn(II) enzyme has a very low catalytic activity.[5,29] Nevertheless, we observe a "pseudo-bidentate" coordination of HCO_3^- with a "normal" (2.2 Å) and a longer (2.5 Å) oxygen–zinc distance and with a carbon–zinc distance of 2.7 Å in closer agreement with the Mn(II) CA estimates than with those on the Co(II) enzyme.

Several theoretical calculations relating to the binding of HCO_3^- in the active site of CA have been performed.[30–36] In most cases it was found that the most stable binding mode involves metal coordination of one or both of the unprotonated oxygen atoms of the ligand so that charge separation is minimized. However, this presents somewhat of a mechanistic dilemma. Recent molecular dynamics and free energy perturbation simulations[37,38] as well as kinetic and crystallographic studies of wild-type (M. Lindahl, L.A. Svensson, and A. Liljas, Proteins, accepted for publication) as well as mutant CA[39] confirm previous suppositions[5] that the CO_2 substrate is not metal coordinated but located in a hydrophobic pocket in the vicinity of the metal ion. The zinc hydroxide mechanism model, therefore, implies that the OH group is closer to the metal ion than the other oxygen atoms of HCO_3^- immediately after reaction of the metal-bound OH^- with CO_2. To circumvent this dilemma various speculative schemes in-

volving reorientation of the HCO_3^- ion have been proposed.[5,40] Furthermore, Liang and Lipscomb[32] calculated that a water-mediated proton transfer between oxygen atoms of HCO_3^- has a very low activation barrier. Thus, these authors proposed that the proton migrates rapidly between the oxygen atoms of HCO_3^-.

Our results suggest a different solution to this problem. If it is assumed that Glu-106 (Fig. 2) is ionized at our experimental conditions in accordance with recent calculations by Merz,[41] the hydroxyl group of Thr-199 must donate its hydrogen to Glu-106 and can only act as an acceptor in its hydrogen bond to the metal-bound bicarbonate ion.[2] This would imply that it is the OH group of HCO_3^- that forms the short (2.2 Å) bond to the metal ion in this enzyme–substrate complex, and no subsequent reorganization or proton transfer has to be invoked.[2] This binding mode for HSO_3^- is analogous to that previously observed for the $R\text{-}SO_2NH^-$ group of acetazolamide[42] and for HCO_3^- (ref. 43 and Håkansson et al., J. Mol. Biol., accepted for publication). Unprotonated anions like SCN^- and formate (ref. 2 and Håkansson et al., J. Mol. Biol., accepted for publication) either bind at a fifth coordination site without displacing the water molecule hydrogen bonded to Thr-199, or like CN^- and OCN^- (Lindahl, et al., Proteins, accepted for publication), displace the deep water at the amide group of Thr-199 and bind near the zinc H_2O/OH^-. These results indicate that Thr-199, together with Glu-106, is very important for the selection and orientation of metal ligands that can also act as hydrogen-bond donors.

Furthermore, this binding mode for HCO_3^- appears to be ideal for catalysis. In the conversion of HCO_3^- to CO_2, there is no need for an energetically unfavorable reorganization of the HCO_3^- ion, and the transition state can be attained with minimal structural rearrangements.

ACKNOWLEDGMENTS

Kjell Håkansson and Martin Lindahl are thanked for help at various stages of this project as well as communicating their results before publication. We would like to thank Prof. I. Bertini for valuable discussions. This work was financially supported by grants from the Swedish Natural Science Research Council to S.L. (K 2911) and to A.L. (K 3262), from NUTEK, and from the Nordic Industrial Fund (J.V.). The crystallographic equipment was obtained due to grants from the Swedish Council for Planning and Coordination of Research (FRN), the SE-bank, and from the Knut and Alice Wallenberg foundation.

REFERENCES

1. Silverman, D.N., Lindskog, S. The catalytic mechanism of carbonic anhydrase: Implications of a rate-limiting proteolysis of water. Acc. Chem. Res. 21:30–36, 1988.
2. Eriksson, E.A., Kylsten, P.M., Jones, T.A., Liljas, A. Crystallographic studies of inhibitor binding sites in human carbonic anhydrase II: A pentacoordinated binding of the SCN^- ion to the zinc at high pH. Proteins 4:283–293, 1988.
3. Tu, C., Silverman, D.N., Forsman, C., Jonsson, B.-H., Lindskog, S. Role of histidine 64 in the catalytic mechanism of human carbonic anhydrase II studied with a site-specific mutant. Biochemistry 28:7913–7918, 1989.
4. Tashian, R.E. The carbonic anhydrases: Widening perspectives on their evolution, expression and function. BioEssays 10:186–192, 1989.
5. Lindskog, S. Carbonic anhydrase. Adv. Inorg. Biochem. 4:115–170, 1982.
6. Behravan, G., Jonsson, B.-H., Lindskog, S. Fine tuning of the catalytic properties of carbonic anhydrase. Studies of a Thr200 → His variant of human isoenzyme II. Eur. J. Biochem. 190:351–357, 1990.
7. Khalifah, R.G., Strader, D.J., Bryant, S.H., Gibson, S.M. Carbon-13 nuclear magnetic resonance probe of active-site ionizations in human carbonic anhydrase B. Biochemistry 16:2241–2247, 1977.
8. Tilander, B., Strandberg, B., Fridborg, K. Crystal structure studies on human erythrocyte carbonic anhydrase C. J. Mol. Biol. 12:740–760, 1965.
9. Howard, A.J., Gilliand, G.L., Finzel, B.C., Poulos, T.L., Ohlendorf, D.H., Salemme, F.R. The use of an imaging proportional counter in macromolecular crystallography. J. Appl. Crystallogr. 20:338–387, 1987.
10. CCP4, 1979. The SERC (UK) collaborative computing project no. 4. A suite of programs for protein crystallography distributed from Daresbury Laboratory, Warrington, WA4 4AD, UK.
11. Jones, T.A. A graphics model building and refinement system for macromolecules. J. Appl. Crystallogr. 11:268–272, 1978.
12. Jones, T.A. FRODO: A graphics fitting program for macromolecules. In: "Computational Crystallography." Sayre, D. (ed.) Oxford: Clarendon Press, 1982: 303–317.
13. Jones, T.A., Zou, J.-Y. Cowan, S.W., Kjeldgaard, M. Improved methods for building protein models in electron density maps and the location of errors in these models Acta Crystallogr. A47:110–119, 1991.
14. Hendricksson, W.A., Konnert, J.H. Incorporation of stereochemical information into crystallographic refinement. In: "Computing in Crystallography." Diamond, R., Ramaseshan, S., Venkatesan, K. (eds.). Bangalore: Indian Institute of Science, 1980: 13.01–13.23.
15. Finzel, B.C. Incorporation of fast Fourier transforms to speed restrained least-squares refinement of protein structures. J. Appl. Crystallogr. 20:53–55, 1987.
16. Luzzatti, P.V. Traitment statistique des erreurs dans la determination des structures cristallines. Acta Crystallogr. 5:802–810, 1952.
17. Eriksson, A.E., Jones, T.A., Liljas, A. Refined structure of human carbonic anhydrase II at 2.0 Å resolution. Proteins 4:274–282, 1988.
18. Simonsson, I., Jonsson, B.-H., Lindskog, S. A ^{13}C nuclear magnetic resonance study of CO_2/HCO_3^- exchange catalyzed by human carbonic anhydrase I. Eur. J. Biochem. 129;165–167, 1982.
19. Ren, X., Lindskog, S. Buffer dependence of CO_2 hydration catalyzed by human carbonic anhydrase I. Biochim. Biophys. Acta, 1120:81–86, 1992.
20. Kannan, K.K., Ramanadham, M., Jones, T.A. Structure, refinement, and function of carbonic anhydrase isoenzymes: Refinement of human carbonic anhydrase I. Ann. N.Y. Acad. Sci. 429:49–60, 1984.
21. Bernstein, F.C., Koetzle, T.F., Williams, G.J.B., Meyer, E.F., Jr., Brice, M.D., Rogers, J.R., Kennard, O., Shimanouchi, T., Tasumi, M. The Protein Data Bank: A computer-based archival file for macromolecular structures. J. Mol. Biol. 112:535–542, 1977.
22. Abola, E.E., Bernstein, F.C., Bryant, S.H., Koetzle, T.F., Weng, J. "Protein Data Bank." In: "Crystallographic Databases—Information Content, Software Systems, Scientific Applications." Allen, F.H., Bergerhoff, G., Sievers, R. (eds.). Bonn/Cambridge/Chester: Data Commission of the International Union of Crystallography, 1987: 107–132.
23. Krebs, J.F., Fierke, C.A., Alexander, R.S., Christianson, D.W. Conformational mobility of His-64 in the Thr-200 →

Ser mutant of human carbonic anhydrase II. Biochemistry 30:9153–9160, 1991.
24. Nair, S.K., Christianson, D.W. Unexpected pH-dependent conformation of His-64, the proton shuttle of carbonic anhydrase II. J. Am. Chem. Soc. 113:9455–9458, 1991.
25. Campbell, I.D., Lindskog, S., White, A.I. A study of the histidine residues of human carbonic anhydrase C using 270 MHz proton magnetic resonance. J. Mol. Biol. 98:597–614, 1975.
26. Campbell, I.D., Lindskog, S., White, A.I. A study of the histidine residues of human carbonic anhydrase B using 270 MHz proton magnetic resonance. J. Mol. Biol. 90:469–489, 1974.
27. Bertini, I., Canti, G., Luchinat, C., Scozzafava, A. Characterization of cobalt (II) bovine carbonic anhydrase II and its derivatives. J. Am. Chem. Soc. 100:4873–4877, 1978.
28. Williams, T.J., Henkens, R.W. Dynamic ^{13}C NMR investigations of substrate interaction and catalysis by cobalt(II) human carbonic anhydrase I. Biochemistry 24:2459–2462, 1985.
29. Led, J.J., Neesgaard, E. Paramagnetic carbon-13 NMR relaxation studies on the kinetics and mechanism of HCO_3^-/CO_2 exchange catalyzed by manganese(II) human carbonic anhydrase I. Biochemistry 26:183–192, 1987.
30. Pullman, A. Carbonic anhydrase: Theoretical studies of different hypotheses. Ann. N.Y. Acad. Sci. 367:340–355, 1981.
31. Cook, C.M., Haydock, K., Lee, R.H., Allen, L.C. Electronic structure investigations of catalysis: Carbonic anhydrase. J. Phys. Chem. 88:4875–4880, 1984.
32. Liang, J.-Y., Lipscomb, W.N. Hydration of carbon dioxide by carbonic anhydrase: Internal proton transfer of Zn^{2+}-bound HCO_3^-. Biochemistry 26:5293–5301, 1987.
33. Vedani, A., Huhta, D.W., Jacober, S.P. Metal coordination, H-bond network formation, and protein-solvent interactions in native and complexed human carbonic anhyhdrase I: A molecular mechanics study. J. Am. Chem. Soc. 111: 4075–4081, 1989.
34. Merz, K.M. Jr., Hoffmann, R., Dewar, M.J.S. Mode of action of carbonic anhydrase. J. Am. Chem. Soc. 111:5636–5649, 1989.
35. Jacob, O., Cardenas, R., Tapia, O. An ab initio study of transition structures and associated products in $[ZnOHCO_2]^+$, $[ZnHCO_3H_2O]^+$, and $[Zn(NH_3)_3HCO_3]^+$ hypersurfaces. On the role of zinc in the catalytic mechanism of carbonic anhydrase. J. Am. Chem. Soc. 112:8692–8705, 1990.
36. Krauss, M., Garmer, D.R. Active site ionicity and the mechanism of carbonic anhydrase. J. Am. Chem. Soc. 113: 6426–6435, 1991.
37. Merz, K.M., Jr. CO_2 binding to human carbonic anhydrase II. J. Am. Chem. Soc. 113:406–411, 1991.
38. Liang, J.-Y., Lipscomb, W.N. Binding of substrate CO_2 to the active site of human carbonic anhydrase II: A molecular dynamics study. Proc. Natl. Acad. Sci. U.S.A. 87: 3675–3679, 1990.
39. Nair, S.K., Calderone, T.L., Christianson, D.W., Fierke, C.A. Altering the mouth of a hydrophobic pocket. Structure and kinetics of human carbonic anhydrase II mutants at residue Val-121. J. Biol. Chem. 266:17320–17325, 1991.
40. Lindskog, S. Carbonic anhydrase. In "Zinc Enzymes." Spiro, T.G. (ed.). New York: Wiley, 1983: 77–121.
41. Merz K.M., Jr. Determination of pK_as of ionizable groups in proteins: The pK_a of Glu 7 and 35 in hen egg white lysozyme and Glu 106 in human carbonic anhydrase II. J. Am. Chem. Soc. 113:3572–3575, 1991.
42. Vidgren, J., Liljas, A., Walker, N.P.C. Refined structure of the acetazolamide complex of human carbonic anhydrase II at 1.9 Å. Int. J. Macromol. 12:342–344, 1990.
43. Lindahl, M., Habash, J., Harrop, S., Helliwell, J.R., Liljas, A. The sensitivity of the Laue method to small structural changes: Binding studies of human carbonic anhydrase II (HCA II). Acta Crystallogr. B48, in press, 1992.